Journal of Neonatal Surgery
ISSN (Online): 2226 -0439
Vol. 14, Issue 7S (2025)
https://www.jneonatalsurg.com

OPEN ACCESS

Enhanced Breast Cancer Treatment Using Orlistat-Loaded Lipid-Polymer Hybrid Nanoparticles: Formulation, Characterization and Evaluation

G. Snehalatha[1*], Shailaja Pashikanti[2]

[1]*Research Scholar, Pharmaceutics Division, A.U. College of Pharmaceutical Sciences, Andhra University, Visakhapatnam-530003, Andhra Pradesh, India
[2]Associate Professor, Pharmaceutics Division, A.U. College of Pharmaceutical Sciences, Andhra University, Visakhapatnam-530003, Andhra Pradesh, India

***Corresponding Author:** G. Snehalatha
*Email: snehalatha.g16@gmail.com

Cite this paper as: G. Snehalatha, et.al (2025) Enhanced Breast Cancer Treatment Using Orlistat-Loaded Lipid-Polymer Hybrid Nanoparticles: Formulation, Characterization and Evaluation" *Journal of Neonatal Surgery*, 14 (7S), 746-759.

Abstract:
Breast cancer continues to be a significant global health concern, prompting the development of advanced drug delivery systems to improve therapeutic effectiveness and minimize adverse effects. Lipid-polymer hybrid nanoparticles (LPHNPs) offer a promising approach by combining the benefits of both liposomes and polymeric nanoparticles, thereby improving drug solubility, bioavailability, and controlled release. This study aimed to develop and optimize Orlistat-loaded LPHNPs (ORL-LPHNPs) using soya lecithin, Eudragit RLPO, and Tween 80 via nanoprecipitation. Various formulations (LPHNP1-LPHNP8) were assessed based on various parameters including particle size, polydispersity index (PDI), Zeta Potential, Entrapment Efficiency (EE), And Drug Loading Capacity (DLC). Among the formulations, LPHNP8 exhibited optimal characteristics, with a particle size of 128±2.7.2 nm, PDI of 0.112±0.09, zeta potential of -33±2.1 mV, EE of 92.07±1.6%, and DLC of 55.24±1.7%. In vitro drug release studies indicated a sustained release pattern, best fitting the Higuchi and Korsmeyer- Peppas models, suggesting a diffusion-controlled release mechanism. Cytotoxicity studies against MCF-7 and MDA-MB-231 breast cancer cell lines exhibited anticancer efficacy of optimized ORL-LPHNPs. Stability studies further confirmed the formulation's robustness over six months. These findings highlight the potential of ORL- LPHNPs as an effective nanocarrier system for breast cancer treatment, warranting further in vivo investigations.

Keywords: Breast Cancer, Hybrid Nanoparticles, Release Kinetics, Stability, Cytotoxicity studies.

INTRODUCTION

Breast cancer remains a significant health concern, being the most commonly diagnosed cancer among women in the United States, excluding skin cancers. Approximately 1 in 8 U.S. women (about 13%) will develop invasive breast cancer over the course of their lifetime. In 2024 alone, an estimated 310,720 women are expected, upon receiving a diagnosis of invasive breast cancer, along with 56,500 new cases of non-invasive (in situ) breast cancer (1). Encouragingly, advancements in early detection and treatment have led to a decline in breast cancer mortality rates. Since 1989, death rates have decreased by 44%, resulting in approximately 518,000 fewer deaths. This improvement is attributed to better screening practices, increased awareness, and the development of more effective treatments. However, recent trends indicate a rise in breast cancer incidence, particularly among younger women. Between 2012 and 2021, diagnoses in women under 50 increased by 1.4% annually. Certain demographics, such as Asian American and Pacific Islander women, have experienced even higher annual increases of 2.5% and 2.7%, respectively. Factors contributing to this uptick may include lifestyle changes, reproductive patterns, and increased screening rates. In addition to affecting women, breast cancer also impacts men, though less frequently. In 2024 An estimated 2,800 males in the United States will be diagnosed with invasive breast cancer, with approximately 530 men succumbing to the illness. The lifetime risk for males developing breast cancer is about 1 in 726 (2). Currently, there are over 4 million breast cancer survivors in the United States, reflecting the progress made in combating this disease. Nonetheless, these statistics underscore the importance of continued research, early detection, and equitable access to treatment to further reduce the impact of breast cancer across all populations. Treatment challenges for breast cancer often arise from issues such as poor drug solubility, low bioavailability, limited Cellular internalization, development of drug resistance, and

systemic adverse effects. These limitations increase Treatment expenses and unwanted side effects. Emerging technologies, particularly nanotechnology, offer promising solutions to these problems. Nanocarriers can minimize systemic toxic effects, thereby reducing therapy costs while improving drug targeting and delivery. By enhancing Systemic distribution of drugs, drug availability, sustained release dynamics, and targeting of specific receptors. Nanocarriers optimize therapeutic outcomes (3). Their Improved permeability and retention effect for more precise targeting of nanoscale drug compounds, increasing deposition in cancer cells while sparing normal cells. Lipid-polymer hybrid nanoparticles (LPHNPs) have surfaced as next-generation (4) nanostructures Incorporating the benefits of both liposomes and polymeric nanoparticles. These core-shell systems feature a lipid coating surrounding a polymeric core loaded with the drug, providing prolonged systemic circulation, protection against drug degradation, and prevention of water infiltration into the drug core. Penetrating the drug core, LPHNPs exhibit notable drug entrapment efficacy, regulated drug release, cellular specificity, and stability in the bloodstream. Presently, there are no studies dedicated to investigating LPHNPs for Orlistat (5).

The present study aimed to develop ORL-loaded lipid-polymer hybrid nanoparticles using Soy Lecithin, Tween 80, and Eudragit RLPO. The nanoparticles were evaluated for their particle size, drug release profile, and anticancer activity against MCF7 and MDA-MB 231 cell lines. This approach is expected to enhance drug loading and anticancer efficacy while reducing toxicity to normal cells.

Materials: Orlistat obtained as gift sample from Lee Pharma Pvt. Ltd. Visakhapatnam. India. Tween 80, Soy lecithin, Eudragit RLPO used analytical grade. Ethanol also used analytical grade. MTT Reagent [M5655] and DMSO [PHR1309] were from Sigma. 96-well plate for culturing cells was from Corning, USA.

Preparation of Calibration Curve in PBS pH 7.4 Buffer:

A quantity of 10 mg of Orlistat was dissolved in a volumetric flask with an appropriate volume of phosphate-buffered saline (PBS) at pH 7.4, and the total volume was adjusted to 10mL. From this initial solution, a 1 mL portion was extracted and further diluted to 10 mL with PBS (pH 7.4), resulting in a secondary solution with a concentration of 100 µg/mL. For the preparation of a series of standard solutions, different volumes (ranging from 0.2 to 2 mL) of the secondary solution were transferred into 10 mL volumetric flasks and diluted up to the mark using PBS. As a result, solutions with concentrations of 2, 4, 6, 8, 10, 12, 14, 16, 18, and 20 µg/mL were obtained and subsequently analyzed at the specified wavelength.

Preparation and Optimization of ORL-lipid Polymer Hybrid Nanoparticles using Nanoprecipitation Method

ORL-Lipid Polymer Hybrid Nanoparticles (LPHNPs) were synthesized through a dual method involving probe sonication and magnetic stirring. The fabrication process began by melting the lipid at 40°C in de-ionized water. Next, Eudragit RLPO and the drug were dissolved in ethanol and introduced into the system by adding the required surfactant. Subsequently, the removal of the organic phase (ethanol) was carried out through stirring, while adjusting the final volume with deionized water. The resulting mixture underwent probe sonication at intermediate amplitude to achieve a dispersion of LPHNs. The 1% W/V of cryoprotectant mannitol is added before lyophilization. Various strategies concerning material ratios were implemented to optimize the nano formulations, with comparisons made based on the particle sizes obtained from LPHNP-1 to LPHNP-8.

Table 1: Formulation of Lipid Polymer Hybrid Nano-Particles using Nanoprecipitation method

Batch code	Drug (mg)	Lipid (mg)	Polymer (mg)	Surfactant (mL)	Stirring Time (min)	Injection Speed	Sonication
LPHNP1	60	60	60	1 ml	40	1ml/min	2
LPHNP2	60	60	120	1 ml	50	1ml/min	4
LPHNP3	60	60	180	1 ml	60	1ml/min	6
LPHNP4	60	60	240	1 ml	70	1ml/min	8
LPHNP5	60	120	60	1 ml	50	1ml/min	4
LPHNP6	60	120	120	1 ml	60	1ml/min	6
LPHNP7	60	120	180	1 ml	70	1ml/min	8
LPHNP8	60	120	240	1 ml	80	1ml/min	10

Compatibility Studies:

Fourier Transform Infrared Spectroscopy (FT-IR)

FTIR analysis was conducted using a Shimadzu FTIR spectrophotometer to evaluate the compatibility between the drug (Orlistat) and the polymer (Eudragit) used in lipid polymer hybrid nanoparticle formulation, including, Tween 80, Soya lecithin as a carrier. The FTIR spectra were recorded a frequency range of 4000–500 cm^{-1} by scanning the samples in the spectrophotometer. This study was performed separately to identify any possible interactions between the drug and the excipients.

Differential Scanning Calorimetry (DSC)

The melting point of the pure drug and its compatibility with lipids were analyzed using a differential scanning calorimeter. DSC analysis was carried out on a Shimadzu DSC-60, with the samples placed in Aluminum crucibles for measurement. This study aimed to assess thermal behavior and potential interactions between the drug and lipid excipients.

Analysis of Characterization results for the Optimizing the best Formulation (8)**.**

The lipid-polymer hybrid nanoparticles (LPHNPs) were characterized by assessing their Particle Size, Polydispersity Index (PDI), Zeta Potential, Surface Morphology, and Drug Entrapment Efficiency. Particle Size and PDI were determined using Dynamic Light Scattering analysis, while Zeta Potential was measured by analyzing electrophoretic mobility with a Zeta Sizer. Additionally, Encapsulation Efficiency (EE) and Drug-Loading Capacity (DLC) were quantified. The average particle size, PDI, and zeta potential of the nano-formulations were obtained from three independent measurements.

Scanning Electron Microscopy (SEM)

Scanning Electron Microscopy (SEM) studies begin by preparing the sample prepared by mounting it onto Aluminium stub is affixed using a conductive adhesive such as carbon tape. The specimen is coated with a delicate layer of conductive material, such as gold or platinum, through sputter-coating to prevent charging upon exposure to the electron beam. The coated specimen is positioned inside the SEM enclosure and pictures are captured by traversing the surface with a precise electron beam, offering insights into the morphology and surface attributes.

Transmission Electron Microscopy (TEM)

For Transmission Electron Microscopy (TEM), the sample is typically prepared either as an ultrathin section, often at the nano-meter scale, or as a dispersion in a compatible solvent and then applied onto a copper grid coated with carbon. The example provided is allowed to dry, and, if necessary, stained with a contrasting agent like uranyl acetate or lead citrate. TEM imaging is performed by transmitting an electron beam through the sample, revealing internal structures, size, and shape at high resolution.

% Entrapment Efficiency (EE)

The total drug added during the formulation process is known, and the encapsulated drug is determined by separating free drug (unentrapped drug) from the nanoparticles using centrifugation. The encapsulated drug is then quantified from the nanoparticle pellet after dissolution in a suitable solvent. High EE reflects efficient drug incorporation into the nanoparticles, reducing drug wastage and enhancing formulation efficacy.

$$\%EE = \frac{Experimental\ Drug\ Content}{Theoritical\ drug\ content} X100$$

% Drug Loading Capacity (DLC)

The weight of nanoparticles is determined after lyophilization or drying, and the encapsulated drug content is quantified. This calculation assesses the proportion of the nanoparticle mass that is the active drug. High DLC ensures that a smaller amount of carrier material is required, improving the drug-to-carrier ratio and making the formulation more efficient for therapeutic use.

$$\%DLC = \frac{Amount\ of\ encapsulated\ drug}{Total\ Amount\ of\ Nanoparticles} X100$$

In Vitro Drug Release and Investigation of Release Kinetics:

The assessment of in vitro drug release for optimized formulations was conducted in phosphate-buffered saline (pH = 7.4) to replicate physiological and lysosomal pH conditions. This was achieved using the dialysis bag technique, where a specified amount of lyophilized LPHNPs (equivalent to 60 mg of drug) was dispersed in 2 mL of the corresponding buffer and inserted into a dialysis bag. The dialysis bag was then immersed in 20 mL of release medium. Samples were collected at specific time intervals and replaced with fresh medium to maintain sink conditions. The collected samples underwent analysis using the UV method, and the drug release was recorded. The in vitro drug release data were analyzed using various kinetic models, including zero order, first order, Higuchi model, and Korsmeyer-Peppas model. Regression analysis was performed, and graphs illustrating each model were generated as required for each equation. The representation of each drug release model is provided below

a) Zero Order Release Kinetics:

The release of drug follows the equation $Q = Q_0 + k_0t$, where Q represents the released or dissolved amount of drug, Q is the initial drug quantity in the solution (typically zero), and k0 is the zero order release constant. A plot was generated for Cumulative % drug release against time.

b) First Order Release Kinetics:

Described by Log C = Log C_0 - k_t/2.303, where C0 is the initial drug concentration, and k is the first order constant. The plot was created for the log cumulative percent released versus time.

c) Higuchi Release Kinetics:

Higuchi's model aimed to correlate drug release rate with physical constants through diffusion laws.

The equation $Q_t = k_h(t)^{0.5}$ was formulated by Higuchi to depict drug release from an insoluble matrix. Here, Q_t refers to the drug amount released at time t and k_h is the rate constant. The graph displayed Cumulative % drug release versus the square root of time.

d) Korsmeyer-Peppas Release Kinetics

Defined by $M_t/M_o = k_t n$, where M_t/M_o denotes the fraction of drug released at time t, k is the rate constant, and n is the release exponent. A plot was constructed for % cumulative log percent permeated against log time.

Stability studies (9)

The stability stabilities of LPHNPs involved short term observation of different characteristics, viz., physical appearance, particle size, %Drug content, % Drug release. The Optimized LPHNPs were evaluated according to ICH guidelines at refrigerating storage conditions i.e. temperature (5±2°C) for a period of 6 months.

Cell cytotoxicity (10)

To conduct the MTT assay, 200 µL of cell suspension in complete culture medium containing 10% FBS was dispensed into each well of a 96-well plate, seeded with 20,000 cells per well. The cells were then incubated for 24 hours to facilitate adhesion and proliferation. Following this initial incubation period, the existing medium was replaced with fresh medium containing varying concentrations of the test compounds: Blank, 0.781, 1.563, 3.125, 6.25, 12.5, 25, 50, and 100 µg/mL. The plate was then placed in a 37°C incubator for 48 hours under a humidified atmosphere with 5% CO_2. Post-treatment, the medium was aspirated, and MTT reagent was added to each well to achieve a final concentration of 0.5 µg/mL (prepared using a 0.2 µm filter sterilization). Subsequently, the plate was shielded from light with aluminum foil and returned to the 37°C incubator for 3 hours. After incubation, the MTT solution was aspirated, and 100 µL of DMSO was added to each well to solubilize the formazan crystals. The absorbance at 570nm was measured using a spectrophotometer (Tecan™ Infinite 200Pro). The MCF-7 and MDA-MB-231 cell lines are commonly employed as representative models for breast cancer research, each embodying distinct molecular subtype.

RESULTS AND DISCUSSIONS

Preparation of Orlistat standard graph using Phosphate Buffer Saline pH-7.4.

Standard graph of Orlistat using phosphate buffer saline 7.4 was plotted from 2 to 20 µg/mL concentration. The absorbance was measured at 204nm by using UV spectrophotometer and standard graph shown in Fig 1.

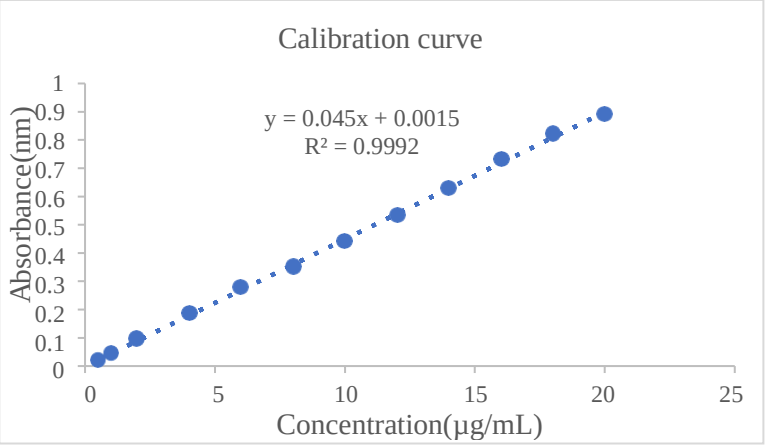

Figure.1 Standard Calibration curve

Table 2: Calibration curve parameters

Parameter	Value
λ_max	204 nm
Beer's Law Limit	10 µg/mL
Equation of Line	Y = 0.045X + 0.0015
Slope (m)	0.045
Intercept (C)	0.0015

R^2 (Correlation Coefficient)	0.992
Standard Deviation (SD)	0.305
Limit of Detection (LOD)	0.223
Limit of Quantification (LOQ)	0.335
Molar Absorptivity (ε)	0.02×10^6 L/mol.cm
Absorbance Mean ($\bar{x}$)	0.419
Confidence Interval (C·I) at 0.05	0.419±0.173
Confidence Interval (C·I) at 0.01	0.419± 0.227

FTIR spectroscopy studies:
FTIR spectroscopy was utilized to investigate potential drug-lipid interactions. The resulting spectra are presented in Figure 2, while Table 3 lists the wavenumbers corresponding to the functional groups of Orlistat. Analysis of the FTIR spectra revealed that the characteristic absorption peaks of Orlistat remained unchanged in its physical mixture with different lipids. Furthermore, no disappearance of Orlistat's vibration bands was observed in these mixtures. This suggests that no chemical interaction occurred between the drug, carrier, and polymers.

Table.3 FTIR Analysis of Orlistat for its Functional Groups and Their Corresponding Wavenumbers

Sl. No	Compound	Wave Number (cm^{-1})	Functional Group
1	Orlistat	1726.31	-C=O stretch
		2919.89	-C-H stretch
		3300.74	-N-H stretch
2	Orlistat: Lecithin	1650.27	-C=O stretch
		2920.31	-C-H stretch
		3412.46	-N-H stretch
3	Orlistat: Eudragit	1640.03	-C=O stretch
		2955.32	-C-H stretch
		3203.78	-N-H stretch
4	Orlistat: Tween 80	1830.55	-C=O stretch
		2856.17	-C-H stretch
		3302.36	-N-H stretch

Differential scanning calorimetry studies:
Differential scanning calorimetry (DSC) was performed to analyze the thermal properties of pure Orlistat and its Optimized formulation. The DSC thermogram of pure Orlistat exhibited a peak at 41.79°C. In the Optimized formulation, the peak was observed at 167°C. These findings indicate that Orlistat remains stable in the presence of different polymers under varying conditions and shows that it is amorphous in nature and the drug completely surrounded by the lipids and polymers showing its greater entrapment. Figure 2 presents the DSC curves of the pure drug and its Formulation.

Factors affecting for optimizing the formulation based on process parameter and based on outcomes of dependent and independent variables (9,11).

Concentration of Lipid:
Optimizing the concentrations of lipids and polymers is crucial in shaping the physicochemical properties, stability, and performance of lipid-polymer hybrid nanoparticles (LPHNPs). Lipids, such as soya lecithin, primarily contribute to the formation of the hydrophobic core, which serves as the drug reservoir. They enhance encapsulation efficiency (EE%) by providing a compatible environment for lipophilic drugs like orlistat. Additionally, lipids improve the stability of nanoparticles by preventing drug leakage and contributing to the structural integrity of the hybrid system.

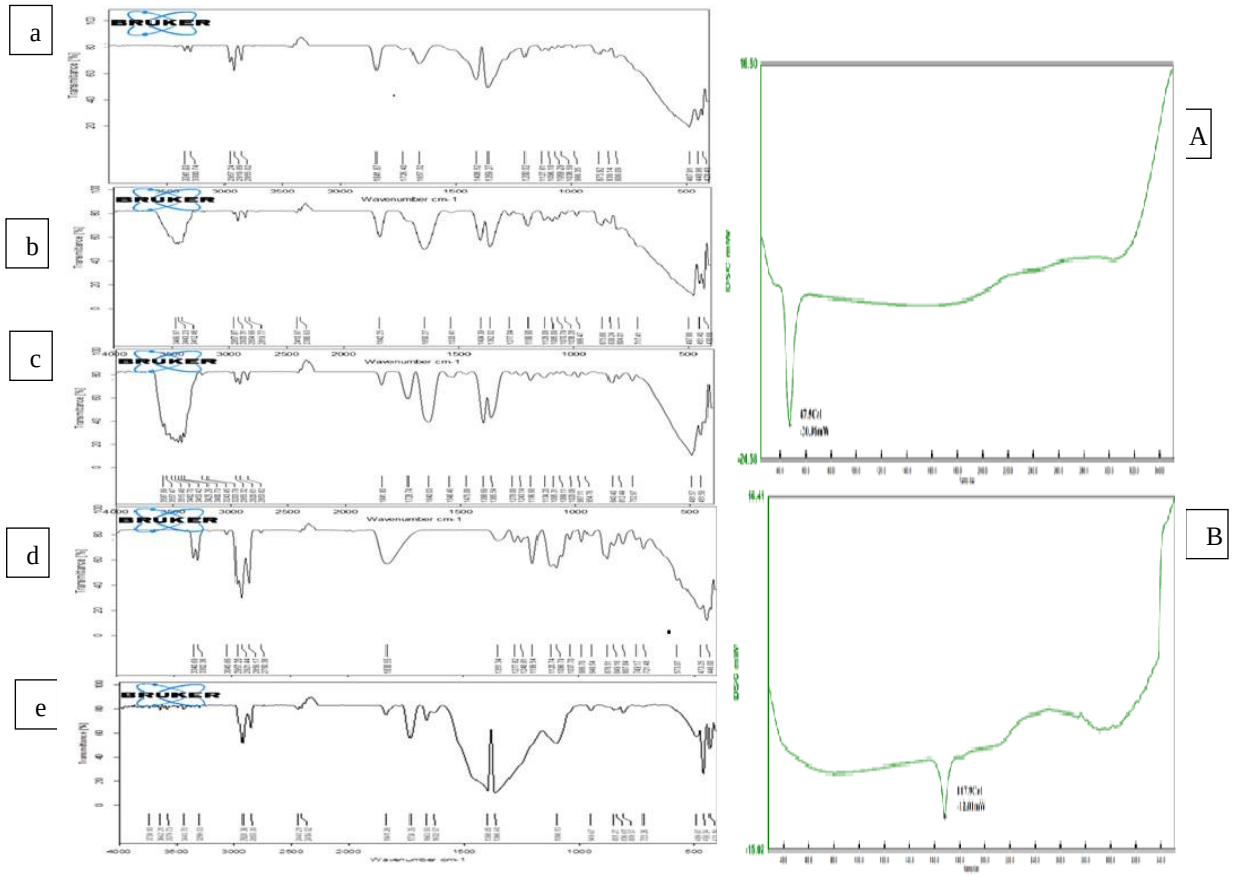

Figure.2 -FTIR Results [a. FTIR Spectra of Orlistat pure drug, b. FTIR Spectra of Orlistat-Soy lecithin, c. FTIR Spectra of Orlistat-Eudragit, d. FTIR Spectra of Orlistat-Tween 80, e. FTIR Spectra of Physical mixture] and DSC Results [A.DSC thermogram of pure Orlistat, B. DSC thermogram of LPHN8 formulation]

Concentration of Polymer:

Polymers, such as Eudragit, form the outer shell or matrix of LPHNPs and are critical for controlling drug release kinetics. The polymeric shell acts as a barrier to diffusion, ensuring sustained and controlled drug release over time. It also provides mechanical strength to the nanoparticles, enhancing their ability to withstand external stresses during storage or administration. The polymer concentration has a substantial impact on the size of particles, zeta potential (surface charge), and polydispersity index (PDI). Higher polymer concentrations can increase particle size due to thicker shell formation, while lower concentrations may lead to unstable particles with irregular morphologies.

Effect of stirring time:

The stirring duration and sonication duration are essential factors in the production of lipid- polymer hybrid nanoparticles (LPHNPs) as they directly influence the physicochemical properties, stability, and overall quality of the formulation. Stirring time is essential during the nanoprecipitation process to ensure the proper mixing of the organic and aqueous phases. Adequate stirring allows the nanoparticles to self-assemble uniformly, leading to a more consistent particle size and a lower polydispersity index (PDI). Insufficient stirring time may result in irregular particle formation, aggregation, and a lack of homogeneity, compromising the stability and efficacy of the nanoparticles.

Effect of sonication time:

Sonication time is equally important, as it facilitates the reduction of particle size and ensures a uniform distribution of particles in the suspension. By applying ultrasonic energy, sonication breaks down larger aggregates into smaller, more stable particles. It also helps eliminate air bubbles and improves ensuring optimal distribution between the lipid and polymer components is essential to attain high encapsulation efficiency (EE%) and drug loading capacity (DLC%). However, excessive sonication can lead to overheating, degradation of sensitive drug molecules, and potential destabilization of the nanoparticle structure.

The relationship between independent variables (Lipid Concentration, Polymer Concentration, Stirring Time, And Sonication Duration) and dependent variables (Particle size, PDI, Z-AVR, Zeta Potential, %EE, and DLC) and among with independent reveals critical trends influencing nanoparticle formulation observed in Table 2, Figure.1 and Figure. 2.

Particle size: Particle size increases with polymer concentration initially (LPHNP1 to LPHNP4) but decreases at higher lipid concentrations and longer sonication times (LPHNP5 to LPHNP8). This indicates that while polymer content promotes particle growth due to aggregation, extended sonication aids in reducing particle size by breaking down larger particles into smaller, uniform ones.

PDI: The PDI values generally decrease with increasing polymer concentration and prolonged sonication (LPHNP1 to LPHNP8). Lower PDI values at higher sonication times suggest improved uniformity in nanoparticle size distribution. The smallest PDI (0.112±0.09) in LPHNP8 confirms optimal conditions for achieving monodisperse nanoparticles.

Z-AVR: Z-AVR trends align with particle size, indicating a correlation between particle aggregation and the hydrodynamic diameter. Larger Z-AVR values are observed at moderate lipid and polymer concentrations but decrease with extended sonication, as seen in LPHNP6 to LPHNP8.

Zeta Potential: Zeta potential values fluctuate across formulations, showing positive and negative charges depending on the balance between lipid and polymer content. The highest zeta potential (12.4 mV) in LPHNP7 suggests greater stability at higher lipid concentrations, while the highly negative zeta potential in LPHNP8 (-33±2.1 mV) indicates improved colloidal stability under those conditions.

Encapsulation Efficiency (EE): EE decreases with increased polymer content up to LPHNP4 but rises significantly in LPHNP8 (92.07±1.6%). This pattern suggests that higher lipid content combined with optimized polymer concentration and sonication enhances drug encapsulation.

Drug Loading Capacity (DLC): DLC follows a similar trend to EE but shows a sharp decline at higher polymer concentrations (LPHNP3 to LPHNP7). LPHNP8 exhibits the highest DLC (55.24±1.7%) among formulations with increased lipid content, signifying the synergistic effect of lipid and sonication in improving drug loading.

The relationships between the Dependent variables can be understood as follows:

Particle Size vs. EE (%) and DLC (%): Smaller particle sizes generally indicate a higher surface area for drug encapsulation, potentially improving encapsulation EE. For example, **LPHNP1** (41.3 nm) and **LPHNP8** (128±2.7.2 nm) show high EE% (89.17% and 92.07±1.6%, respectively), while **LPHNP6** (100.9 nm) exhibits a lower EE% of 78.28%. However, DLC is affected by particle size non-linearly, as seen in **LPHNP8** (128±2.7.2 nm, DLC 55.24±1.7%) being better than smaller **LPHNP6** (100.9 nm, DLC 28.43%).

PDI vs. EE (%) and DLC (%): Polydispersity index (PDI) reflects particle size uniformity. Lower PDI values generally correlate with stable formulations and consistent drug encapsulation. **LPHNP8** (PDI 0.112±0.09) achieves the highest EE% (92.07±1.6%), suggesting that lower PDI may favor encapsulation efficiency. Conversely, higher PDI formulations, like **LPHNP1** (PDI 0.493), still achieve high EE%, indicating additional influencing factors.

Zeta Potential vs. EE (%) and DLC (%): Zeta potential indicates surface charge and stability. High absolute zeta potential values suggest better particle dispersion and stability. **LPHNP8** has a very negative zeta potential (-33±2.1 mV) and achieves the highest EE%, suggesting a correlation between charge and encapsulation efficiency. **LPHNP4** and **LPHNP7**, with positive zeta potentials (11.6 mV and 12.4 mV, respectively), also show good EE%, indicating that stability might not always depend solely on charge.

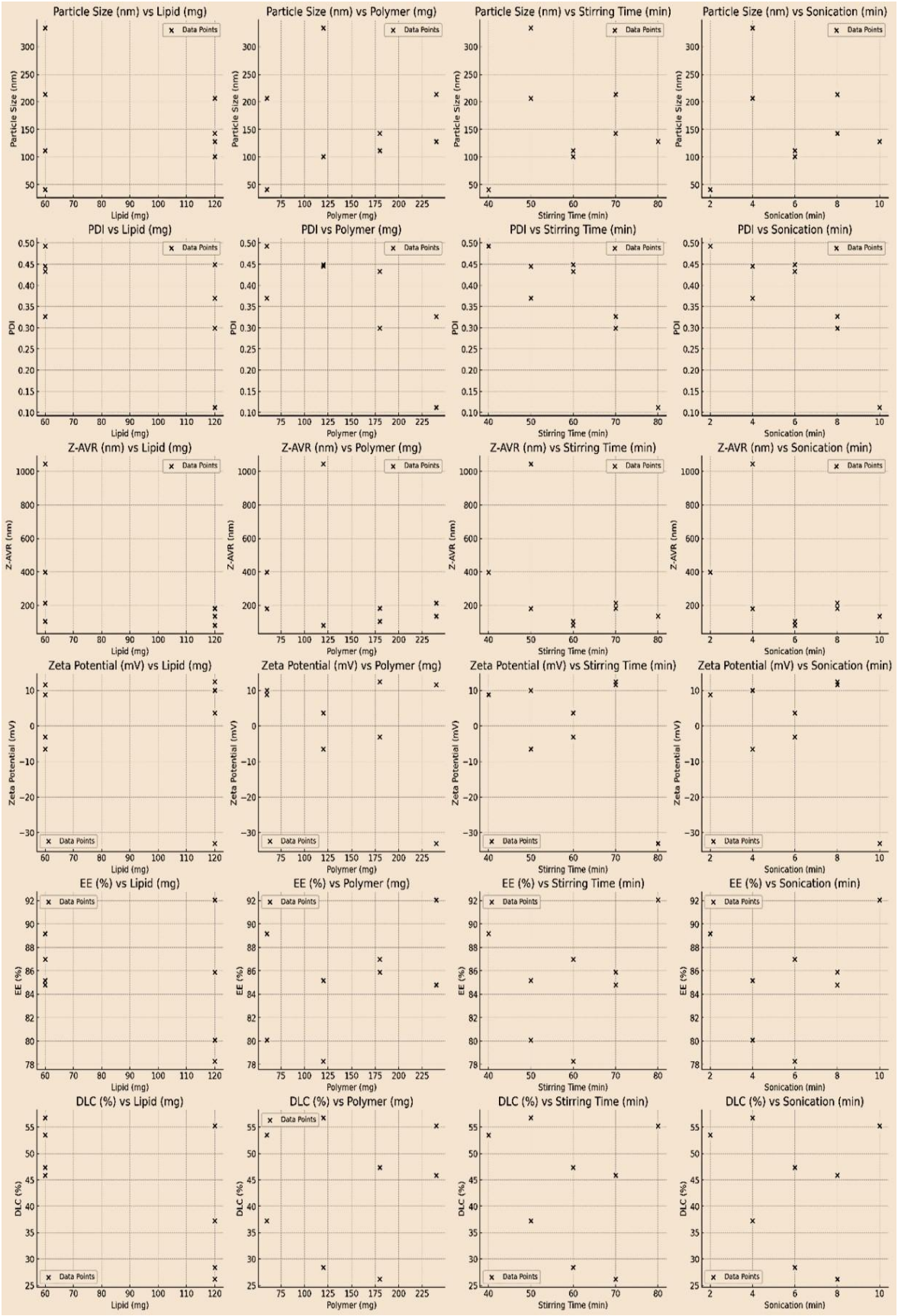

Figure 3: Indicating the factors of dependent variables influenced by independent Variables

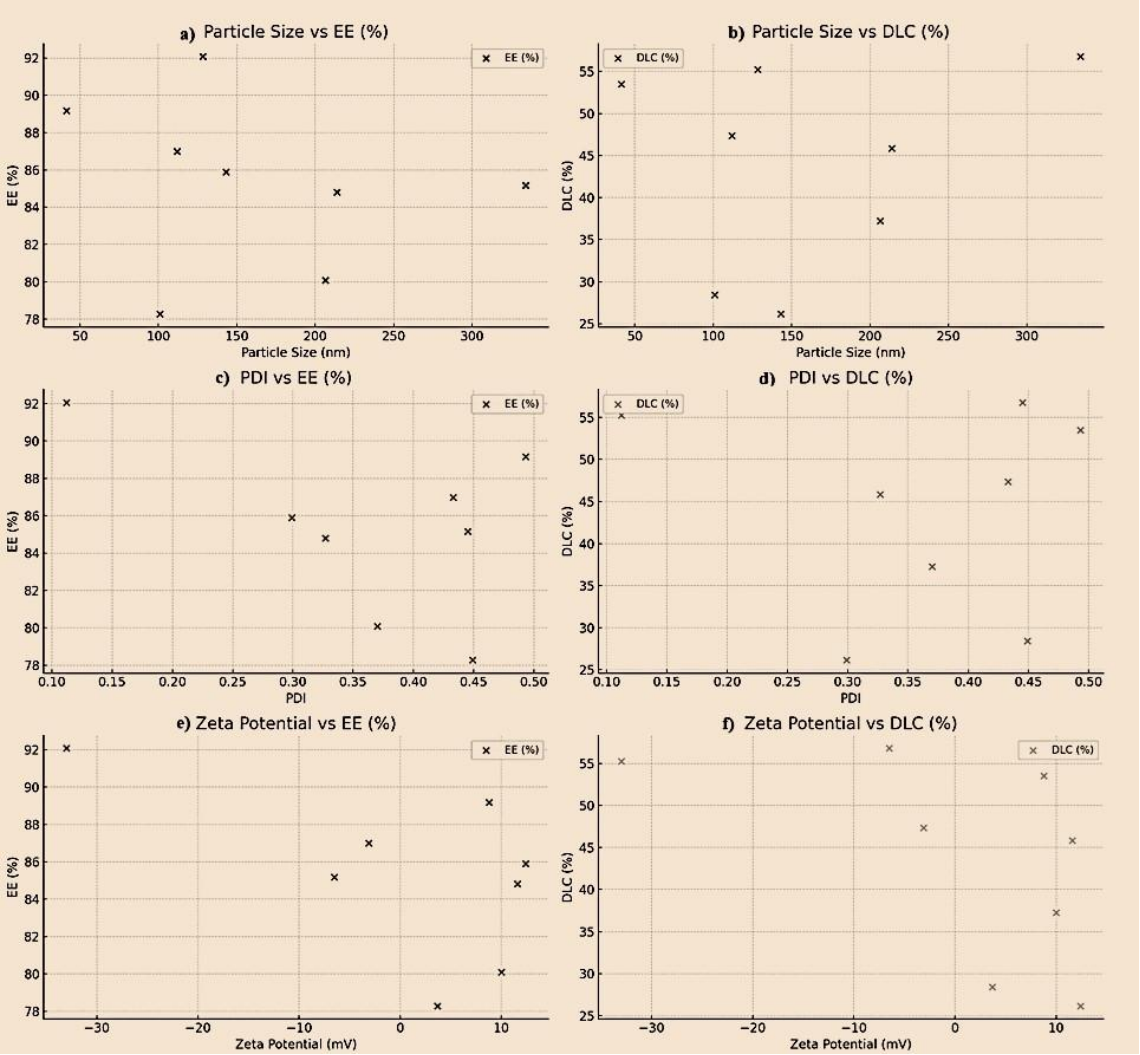

Figure 4: Indicating the influence of dependent factors on one-another

Table 4: Surface morphology and Characterization results

Batch code	Particle size (nm)	PDI	Z-AVR (nm)	Zeta-Potential (Mv)	EE (%)	DLC (%)
LPHNP1	41.3±3.5	0.493±0.12	398.4±45.2	8.8±1.2	89.17±2.7	53.50±1.7
LPHNP2	334.1±2.1	0.445±0.15	145.5±12.3	-6.5±1.3	85.17±2.1	56.78±1.3
LPHNP3	111.9±4.5	0.433±0.13	103.21±7.6	-3.1±1.2	86.99±1.9	47.36±1.5
LPHNP4	213.9±3.9	0.327±0.13	213±14.6	11.6±2.1	84.81±2.2	45.84±1.6
LPHNP5	206.4±4.6	0.370±0.12	180.9±17.1	10±2.3	80.09±2.3	37.25±1.2
LPHNP6	100.9±1.2	0.449±0.14	79.7±8.2	3.7±1.1	78.28±1.8	28.43±1.2
LPHNP7	143±5.8	0.299±0.10	181.5±13.7	12.4±2.4	85.90±1.2	26.16±1.3
LPHNP8	128±2.7	0.112±0.09	135.6±5.2	-33±2.1	92.07±1.6	55.24±1.7

Among all formulations, LPHNP8 demonstrated the most optimal values, adhering to standard ranges for each parameter as High EE% formulations like **LPHNP8** exhibit relatively low DLC. Optimizing the drug-to-lipid/polymer ratio might help improve DLC without sacrificing EE%. **LPHNP8** as a starting point for further refinement. Its parameters (Particle Size: 128±2.7.2 nm, PDI: 0.112±0.09, ZP: -33±2.1, EE%: 92.07±1.6, DLC%:55.24±1.7) Shown in Figure.4, Figure 5 and Table 4 indicating a promising formulation that can be enhanced further for specific needs.

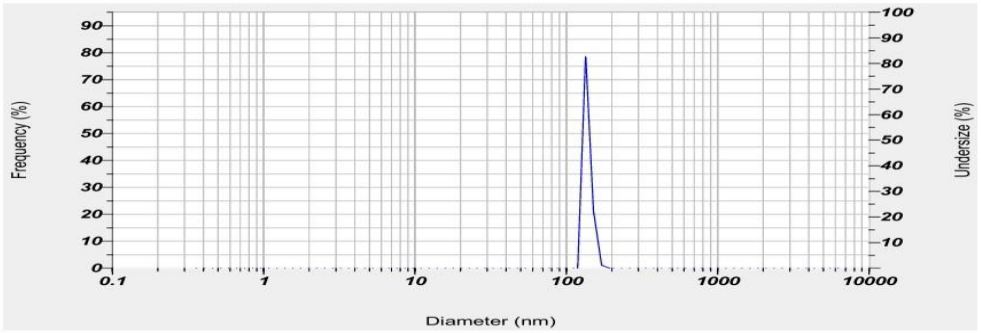

Figure 5: Dynamic light scattering (DLS) image of LPHNP8 NPs distribution by volume of particles (DLS) using HORIBA Scientific Nanoparticle analyzer SZ-100

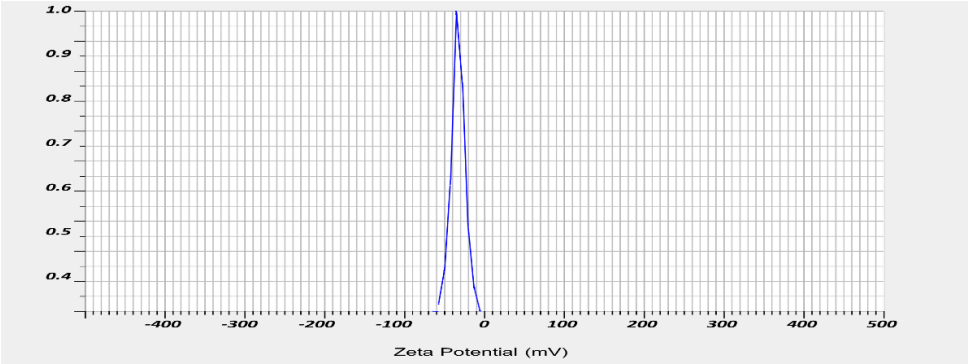

Figure 6. Zeta-Potential analysis of Optimized formulations

This was achieved using nanoprecipitation technique was employed to prepare orlistat-loaded lipid-polymer hybrid nanoparticles. The organic phase was created by dissolving 60 mg of orlistat and 240 mg of Eudragit (polymer) in a 10% v/v ethanol solution. For the aqueous phase, 45 mL of distilled water with 1 millilitre of Tween 80 (2% w/v) was prepared 120 mg of soya lecithin (lipid). The organic phase was subsequently introduced into the aqueous phase at a consistent rate of 1 mL/min using a syringe pump while stirring at 500–1000 rpm. The stirring was continued for 80 minutes at room temperature to facilitate the self-assembly and stabilization of nanoparticles. Subsequently, the mixture sample underwent sonication for 10 minutes with a probe sonicator at an intermediate frequency to reduce particle size and achieve a uniform dispersion. The final suspension volume was adjusted to 50 mL with distilled water. Freeze-drying, or lyophilization, was carried out to enhance the stability of the prepared formulations and facilitate their conversion into dry powder. Prior to lyophilization, cryoprotectant (10%) was added to the samples, followed by overnight cooling at -80°C. The ORL-LPHNs were then placed in the freeze dryer for lyophilization at -75°C for approximately 2 days (48 hours), with the temperature gradually increasing by about 5°C per hour.

SEM and TEM Results:

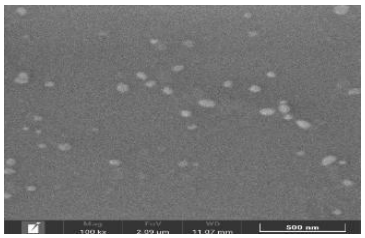

Figure 7: SEM image of LPHNP8

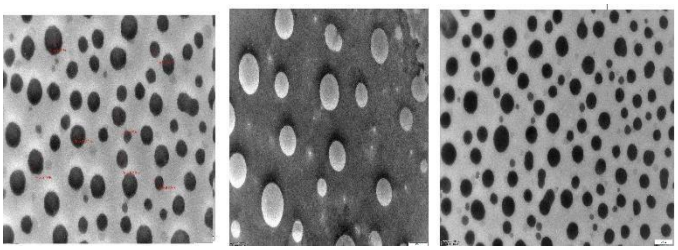

Figure 8: TEM images of LPHNP8 formulation Entrapment

Scanning Electron Microscopy (SEM) and Transmission Electron Microscopy (TEM) studies are conducted to characterize the morphological and structural properties of nanoparticles. SEM provides detailed surface topography for 128±2.7.2 nm size and particle size distribution of 0.112±0.09, enabling the observation of uniformity, shape, and aggregation tendencies. TEM, on the other hand, offers high-resolution imaging to analyzed the structure as round with smooth surface of nanoparticles shown in Figure 7 and Figure 8. These techniques are essential for confirming the successful fabrication of lipid-polymer hybrid nanoparticles (LPHNPs) and ensuring their structural integrity.

Efficiency and Drug Loading Capacity:

LPHNP8 exhibited exceptional encapsulation efficiency (EE) of 92.07±1.6%, ensuring effective drug incorporation into the nanoparticle matrix while minimizing wastage and maximizing therapeutic potential. This high EE highlights the compatibility of orlistat with the lipid-polymer hybrid system in LPHNP8. Additionally, the formulation achieved a remarkable drug-loading capacity (DLC) of 55.24±1.7%, one of the highest among comparable formulations. Such a high DLC reduces dosing frequency. This efficiency is attributed to the optimized ratio of lipid, polymer, and surfactant, which enables effective drug entrapment within the nanoparticle matrix, underscoring the advanced design and therapeutic promise of LPHNP8 in Table- 4.

***In-Vitro* Drug Release:**

Table 5: % Cumulative drug release of Optimized formulation LPHNP8

Time (Hr)	% Cumulative Drug Release at 24hrs
0.5	4.69±1.2
1	10.89±1.5
2	18.13±0.1
3	25.48±0.2
4	32.98±0.4
5	40.96±0.6
6	50.13±0.2
7	59.59±0.6
8	69.46±0.8
12	82.30±1.1
24	95.24±0.6

Each value represents Mean ± S. D. (n=3)

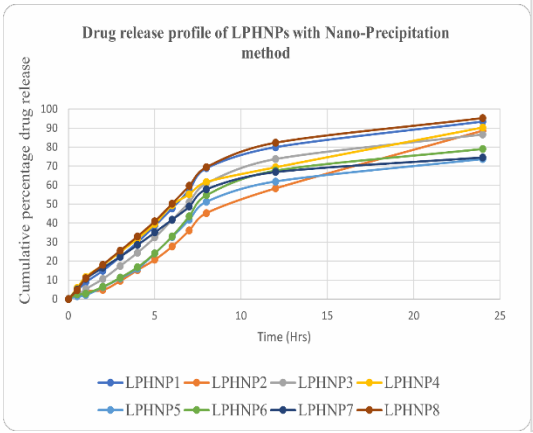

Figure 9: *In-Vitro* Drug Release profile of formulations (LPHNPs1-8)

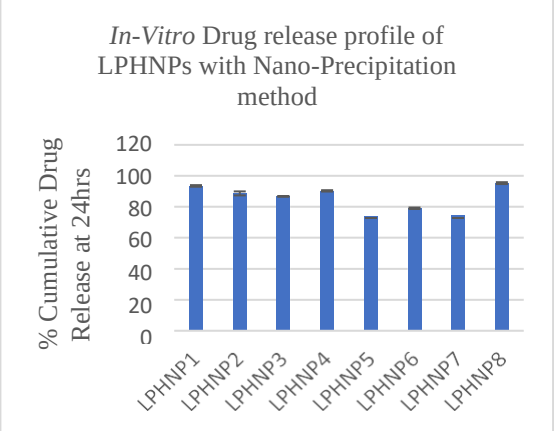

Figure 10: % Cumulative Drug Release at 24th hr for formulations (LPHNPs1-8)

The *In-Vitro* release profile of LPHNP8 demonstrates its efficient drug release shown in table 5. Figure 9 and Figure 10, Shows the graphs of % cumulative drug release of all formulation batches influenced by its formulation parameters and excipients over in time of 24 hrs. The release data of LPHNP8 aligns best with the Higuchi model ($R^2 = 0.986$), indicating diffusion- controlled drug release, which is further supported by the Korsemeyer-Peppas model ($R^2 = 0.965$, n = 0.779), suggesting a non-Fickian (anomalous) release mechanism involving both diffusion and erosion in table 6. The high encapsulation efficiency (92.07±1.6%) and optimized particle size (128±2.7.2 nm) contributed to sustained release, ensuring effective drug delivery. The lipid-polymer hybrid matrix, comprising lipid for controlled release and polymer for stability, plays a critical role in achieving these kinetics. Excipients such as surfactants enhanced emulsification and minimized aggregation, ensuring uniform particle dispersion and efficient drug entrapment. The first-order model ($R^2 = 0.975$) further suggests concentration-dependent drug release shown in Figure 11. These findings highlight how the formulation's characteristics and excipient synergy enable prolonged and controlled drug delivery for therapeutic applications.

Table 6: Release kinetics models of LPHNPs (1-8) and their regression values

Batch code	Zero order		First order		Higuchi	Korsemeyer-Peppas	
	K_0	R^2	K_1	R^2	R^2	R^2	n
LPHNP1	4.121	0.940	0.049	0.995	0.978	0.814	0.997
LPHNP2	4.086	0.950	0.039	0.992	0.960	0.929	1.354
LPHNP3	3.910	0.953	0.036	0.994	0.968	0.897	1.119
LPHNP4	3.699	0.938	0.038	0.975	0.980	0.745	0.902
LPHNP5	3.409	0.961	0.025	0.992	0.947	0.950	1.195
LPHNP6	3.658	0.963	0.029	0.987	0.939	0.924	1.127
LPHNP7	3.213	0.914	0.025	0.982	0.986	0.755	0.889
LPHNP8	4.128	0.935	0.052	0.975	0.921	0.779	0.965

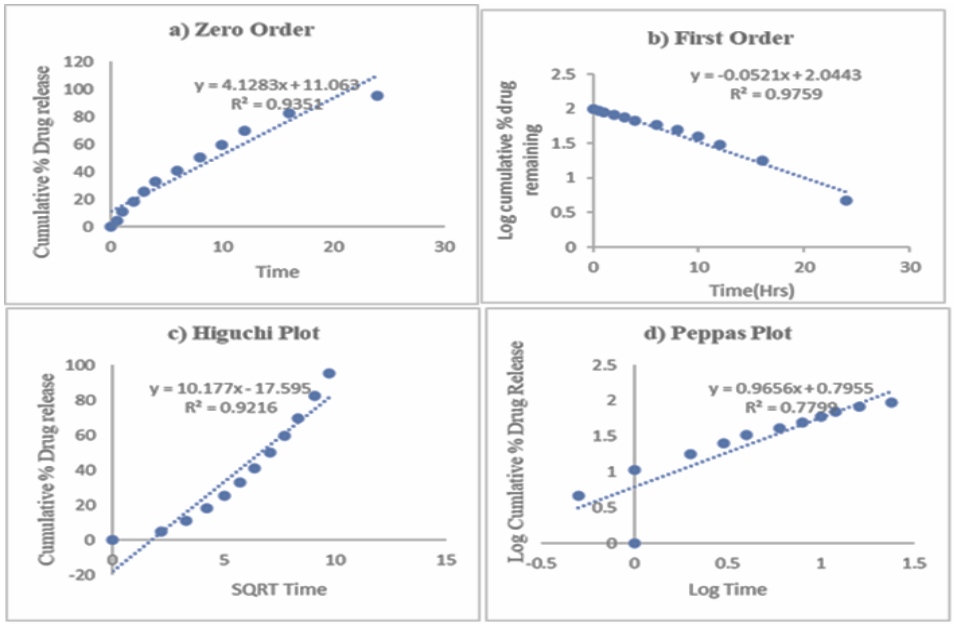

Figure 11: Kinetic models of Optimized formulation LPHNP8

Stability Study Results (12)

The stability stabilities of LPHNPs involved short term observation of different characteristics, viz., physical appearance, particle size, %Drug content, % Drug release. The NPs were evaluated according to ICH guidelines at three different storage conditions i.e. elevated temperature (5±2°C) in refrigerator for a period of 6 months. Equally important, which include the stability of the nanoparticles during storage, the uniformity of the drug distribution within the formulation, and the reproducibility of the drug content in different batches. Analytical techniques like UV spectroscopy or HPLC must be validated to accurately quantify the drug, ensuring that the measured content aligns with the theoretical amount. High drug content (99%) implies efficient encapsulation, proper stabilization of nanoparticles, and minimal degradation or loss of Orlistat during processing and storage shown in Table 7.

Table 7: Stability Study Results

Stability study for Optimized formulation LPHNP8			
Parameters	**Stability at (5 ±2^{0}C) at refrigerator conditions**		
	1 month	**3 months**	**6 months**
Physical appearance	No color change	No color change	No color change
Particle size (nm)	128	128.2	129
% Drug content	55.1	54	54
% Drug release	95.0	94.8	94.1

Particle size remains relatively stable across all time points, indicating good physical stability. Drug content decreases slightly over time, suggesting minimal degradation or loss of active pharmaceutical ingredients. Similarly, drug release shows a marginal decline over 6 months, reflecting sustained drug delivery properties with minimal compromise in release efficiency is observed. Overall, the formulation exhibits robust stability and controlled drug release over an extended period, making it suitable for long-term therapeutic applications.

Cytotoxicity Studies:

Orlistat, a lipase inhibitor, demonstrates its cytotoxic impacts on MCF-7 and MDA-MB-231 cells through distinct mechanisms related to lipid metabolism. In cancer cells, lipogenesis is upregulated to meet the demands of rapid proliferation. This inhibition induces apoptosis and reduces cell viability. The heightened sensitivity of MDA-MB-231 cells in contrast to MCF- 7 cells may stem from the increased reliance of triple-negative breast cancer (MDA-MB-231) cells on FASN activity for survival and proliferation. Morphological changes in cells are often observed during cytotoxic activity and provide valuable insights into the mechanism of action of Orlistat. By inhibiting fatty acid synthase (FASN), Orlistat disrupts lipid biosynthesis, which is crucial for maintaining cellular membrane integrity and structure. This disruption can lead to noticeable changes in cell morphology, including cell shrinkage, loss of adherence, and membrane blebbing—hallmarks of apoptosis. Additionally, cells may exhibit irregular shapes, fragmentation, or disintegration into apoptotic bodies, particularly at higher drug concentrations as shown in Figure 12. Over 48 hours, such changes are more pronounced in MDA-MB-231 cells due to their higher sensitivity to Orlistat. These morphological alterations, such as cellular debris formation, align with Orlistat's interference in lipid metabolism and induction of apoptotic pathways, further emphasizing its potent cytotoxic effects. Figure 13 represents the comparative cytotoxicity effects of the formulated orlistat- loaded lipid-polymer hybrid nanoparticles (ORL-LPHNPs) on MCF-7 and MDA-MB-231 breast cancer cell lines. The first graph illustrates the percentage mean viability of both cell lines across a range of concentrations (0.781–100 µg/mL). A dose-dependent decline in cell viability is observed, with MDA-MB-231 cells showing slightly higher sensitivity to the treatment compared to MCF-7 cells, especially at higher concentrations. This suggests that the nanoparticles exhibit potent anticancer activity, with greater cytotoxic effects on triple- negative breast cancer (MDA-MB-231) cells. Figure 14 depicts the percentage viability of both cell lines over 48 hours of exposure to varying concentrations of ORL-LPHNPs (0.781–100 µg/mL). A gradual reduction in cell viability is evident with increasing drug concentration, reinforcing the dose-dependent cytotoxic response. Notably, MCF-7 cells exhibit slightly higher resistance compared to MDA-MB-231 cells, as reflected in their higher viability at intermediate concentrations. The results highlight the sustained and enhanced anticancer efficacy of ORL-LPHNPs, demonstrating their potential for targeted breast cancer therapy.

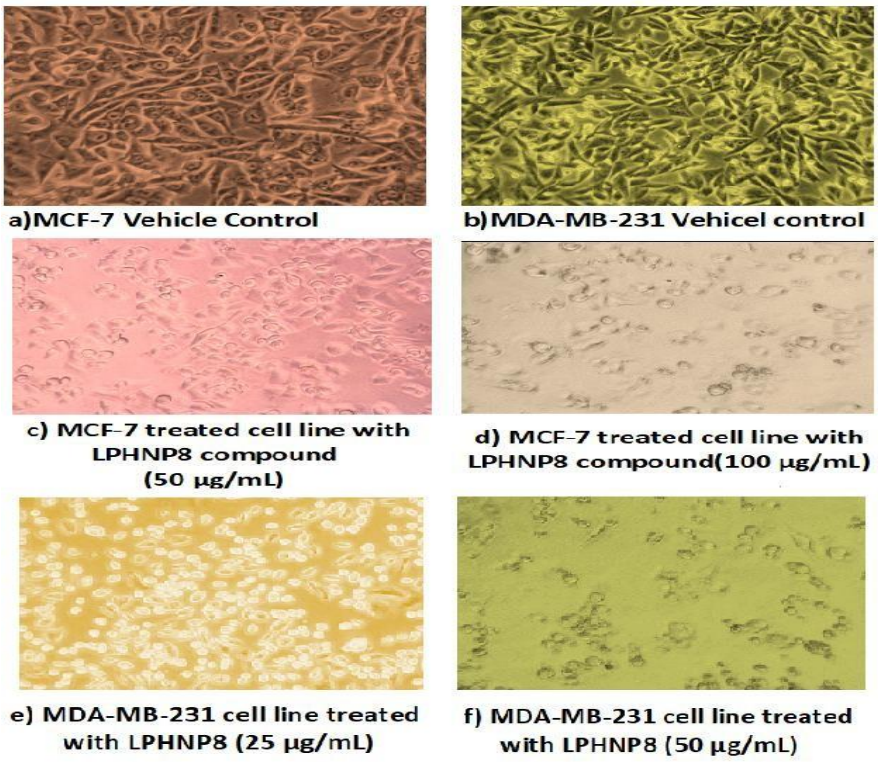

Figure 12: Morphology of Cancer cells after treatment for 48hrs

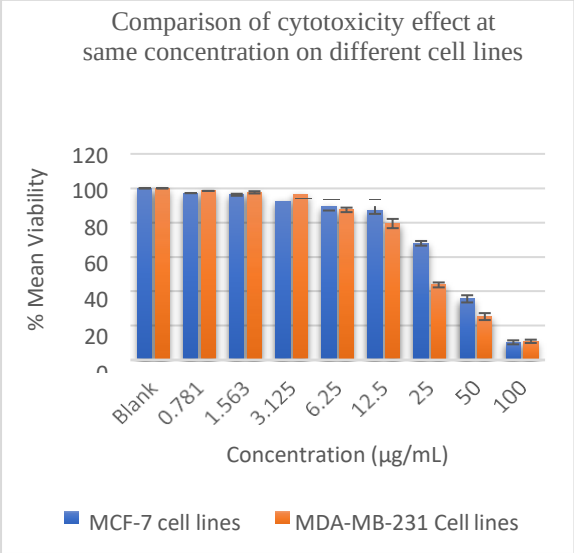

Figure 13: Comparison of cytotoxicity effect at concentration on cell lines

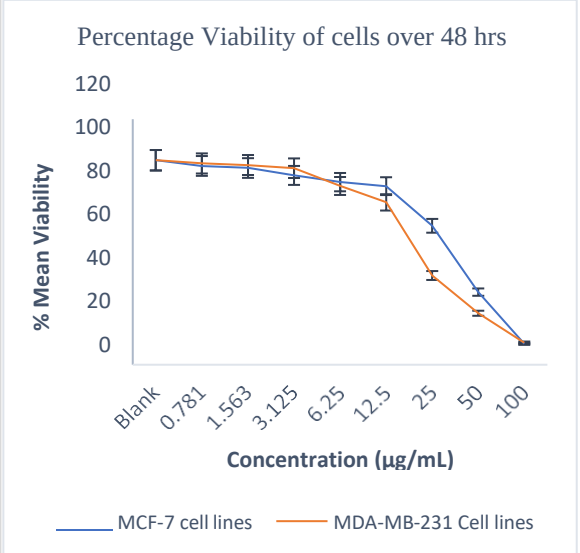

Figure 14. Percentage Viability of cells over 48 hrs

Conclusion

This study successfully formulated and characterized orlistat-loaded lipid-polymer hybrid nanoparticles (ORL-LPHNPs) with enhanced drug encapsulation, release, and shown better anticancer efficacy. The optimized formulation, LPHNP8, exhibited superior physicochemical properties, demonstrating its potential by improving solubility for drug delivery. In vitro drug release studies indicated sustained and controlled release, while cytotoxicity assessments confirmed therapeutic effects against breast cancer cell lines. Stability studies further validated the formulation's long-term viability. These results collectively suggest that ORL-LPHNPs represent a promising strategy for breast cancer treatment, offering a novel and effective approach to overcoming conventional chemotherapy limitations.

References:

1. National Breast Cancer Foundation. Breast Cancer Facts & Stats 2024 - Incidence, Age, Survival, & More. Available from: https://www.nationalbreastcancer.org/breast-cancer-facts/
2. Menon G, Alkabban FM, Ferguson T. Breast Cancer. In: StatPearls. Treasure Island (FL): StatPearls Publishing; Available from: http://www.ncbi.nlm.nih.gov/books/NBK482286/
3. Mohanty A, Uthaman S, Park IK. Utilization of polymer-lipid hybrid nanoparticles for targeted anti-cancer therapy. Molecules. 2020 Oct 1;25(19).
4. Mukherjee A, Waters AK, Kalyan P, Achrol AS, Kesari S, Yenugonda VM. Lipid-polymer hybrid nanoparticles as a nextgeneration drug delivery platform: State of the art, emerging technologies, and perspectives. International Journal of Nanomedicine. 2019; 14:1937–52.
5. Shekhawat R, Mandal CC. Anti-Obesity Medications in Cancer Therapy: A Comprehensive Insight. Current Cancer Drug Targets. 2021 Mar 23;21(6):476–94.
6. Tahir N, Haseeb MT, Madni A, Parveen F, Khan MM, Khan S, et al. Lipid Polymer Hybrid Nanoparticles: A Novel Approach for Drug Delivery. Available from: www.intechopen.com
7. Jain S, Kumar M, Kumar P, Verma J, Rosenholm JM, Bansal KK, et al. Lipid–Polymer Hybrid Nanosystems: A Rational Fusion for Advanced Therapeutic Delivery. Journal of Functional Biomaterials. 2023 Sep 1;14(9).
8. Sivadasan D, Sultan MH, Madkhali O, Almoshari Y, Thangavel N. Polymeric lipid hybrid nanoparticles (Plns) as emerging drug delivery platform—a comprehensive review of their properties, preparation methods, and therapeutic applications. Pharmaceutics. 2021 Aug 1;13(8).
9. Cheow WSH Kunn. Factors affecting drug encapsulation and stability of lipid-polymer hybrid nanoparticles. Colloids and surfaces B, Biointerfaces. 2011;85(2):214–20.
10. Menendez JA, Vellon L, Lupu R. Antitumoral actions of the anti-obesity drug orlistat (Xenical™) in breast cancer cells: Blockade of cell cycle progression, promotion of apoptotic cell death and PEA3-mediated transcriptional repression of Her2/neu (erbB-2) oncogene. Annals of Oncology. 2005;16(8):1253–67.
11. Ansari, Mohammad Javed. "Factors affecting preparation and properties of nanoparticles by nanoprecipitation method." (2018).
12. Q 1 A (R2) Stability Testing of new Drug Substances and Products. ICH topic www.ema.europe.eu/en/documents/scientific-guideline/ich-q-1-r2-stability-testing-new- drug- substance-products-step-5_en.pdf.